

This article was downloaded by:

On: 25 January 2011

Access details: *Access Details: Free Access*

Publisher *Taylor & Francis*

Informa Ltd Registered in England and Wales Registered Number: 1072954 Registered office: Mortimer House, 37-41 Mortimer Street, London W1T 3JH, UK



## Separation Science and Technology

Publication details, including instructions for authors and subscription information:

<http://www.informaworld.com/smpp/title~content=t713708471>

### Gas-Solid Chromatography of Methane-Helium Mixtures: Transmission of a Step Increase in the Concentration of Methane through an Activated Carbon Adsorber Bed at 25°C

Jan-Chan Huang<sup>a</sup>; Robert Forsythe<sup>a</sup>; Richard Madey<sup>a</sup>

<sup>a</sup> DEPARTMENT OF PHYSICS, KENT STATE UNIVERSITY KENT, OHIO

**To cite this Article** Huang, Jan-Chan , Forsythe, Robert and Madey, Richard(1981) 'Gas-Solid Chromatography of Methane-Helium Mixtures: Transmission of a Step Increase in the Concentration of Methane through an Activated Carbon Adsorber Bed at 25°C', *Separation Science and Technology*, 16: 5, 475 — 486

**To link to this Article:** DOI: 10.1080/01496398108068533

URL: <http://dx.doi.org/10.1080/01496398108068533>

## PLEASE SCROLL DOWN FOR ARTICLE

Full terms and conditions of use: <http://www.informaworld.com/terms-and-conditions-of-access.pdf>

This article may be used for research, teaching and private study purposes. Any substantial or systematic reproduction, re-distribution, re-selling, loan or sub-licensing, systematic supply or distribution in any form to anyone is expressly forbidden.

The publisher does not give any warranty express or implied or make any representation that the contents will be complete or accurate or up to date. The accuracy of any instructions, formulae and drug doses should be independently verified with primary sources. The publisher shall not be liable for any loss, actions, claims, proceedings, demand or costs or damages whatsoever or howsoever caused arising directly or indirectly in connection with or arising out of the use of this material.

## Gas-Solid Chromatography of Methane-Helium Mixtures: Transmission of a Step Increase in the Concentration of Methane through an Activated Carbon Adsorber Bed at 25°C

JAN-CHAN HUANG, ROBERT FORSYTHE, and  
RICHARD MADEY

DEPARTMENT OF PHYSICS

KENT STATE UNIVERSITY

KENT, OHIO 44242

### Abstract

Time-dependent transmission or "breakthrough" curves of methane in helium flowing through an activated carbon adsorber bed were measured for methane concentrations between 34 and 105 ppm, and for mixture flow rates between 0.69 and 6.64 cm/s. The transmission is the ratio of the outlet concentration to the inlet concentration. The experimental transmission curves for a step-function increase in the methane concentration are compared with the predictions from a model which assumes a linear adsorption isotherm and equilibrium between the gas and solid phases. These two basic assumptions are discussed in detail. The data show that the two assumptions hold within the concentration and flow rate regions of this study. Effective diffusion coefficients of methane were calculated from the transmission data and found to increase with increasing flow rates.

### INTRODUCTION

The study of the transmission or "breakthrough" curve of a contaminant gas in a carrier gas flowing through a fixed adsorber bed is important in studies of the dynamics of chromatography (1, 2). From a measurement of a transmission curve, one can determine two parameters that characterize the gas-adsorbent system: the effective diffusion coefficient, which is a dynamic property, and the isothermal adsorption capacity, which is a static property (3, 4). The use of the transmission curve offers a convenient way to determine adsorption capacities of gases on a solid adsorbent in the region of low partial pressures (5, 6). The mathematical equations

describing the adsorption and desorption processes can be applied also to other studies such as liquid chromatography (7) and ion-exchange chromatography (8). In all of these applications, the dispersion process is an important factor that determines the performance of the technique. The fact that the contaminant gas flows around the granules of the adsorbent results in paths of different lengths with a consequent distribution of retention times. Some other effects, such as the Brownian motion of the contaminant in the carrier gas and the mass-transfer resistance between the carrier gas and the solid adsorbent, can also contribute to the dispersion process (9). For a constant carrier-gas flow, the dispersion phenomenon can be described by a one-dimensional partial differential equation (10-12):

$$\frac{\partial c}{\partial t} = D \frac{\partial^2 c}{\partial z^2} - u \frac{\partial c}{\partial z} - \frac{1 - \varepsilon}{\varepsilon} \frac{\partial q}{\partial t} \quad (1)$$

Here the phenomenological parameter  $D$  represents the effective diffusion coefficient along the bed length coordinate  $z$ . The concentration  $c(z, t)$  of the contaminant in the gas phase is a function of time  $t$  and  $z$ ,  $u$  is the interstitial flow velocity of the gas mixture,  $q$  is the average concentration of the contaminant gas in the adsorbent which includes the pore volume, and the void volume fraction  $\varepsilon$  includes only the volume external to the adsorbent particles.

For a step increase in the concentration of the contaminant, the initial and boundary conditions are

$$c(x, 0) = 0 \quad (2a)$$

$$c(0, t) = c_0 \quad (2b)$$

$$c(\infty, t) = 0 \quad (2c)$$

By selecting suitable flow rates and maintaining a low partial pressure for the contaminant gas in the carrier gas, we can achieve a linear equilibrium relation between the concentrations of the contaminant in the gas and solid phases; i.e.,

$$q = K'c = [K(1 - \varepsilon_p) + \varepsilon_p]c \quad (3a)$$

and

$$K = \frac{K' - \varepsilon_p}{1 - \varepsilon_p} \quad (3b)$$

Here  $K$  and  $K'$  are dimensionless adsorption capacities, and  $\varepsilon_p$  is the pore volume fraction within the adsorbent granules. The true adsorption capacity  $K$  is the volume of gas adsorbed per unit volume of the solid

adsorbent (which does not include the pore volume), whereas the apparent adsorption capacity  $K'$  is the gas volume adsorbed per unit volume of adsorbent (which includes the pore volume but not the interstitial volume). Note that the introduction of  $\varepsilon_p$  separates the true adsorption capacity  $K$  from the apparent adsorption capacity  $K'$ . The factor  $\varepsilon_p c$  in the right-hand member of Eq. (3a) represents the contaminant in the pore volume; the factor  $K(1 - \varepsilon_p)c$  is the contaminant adsorbed on the solid.

The analytical solution of Eq. (1) with the initial and boundary conditions (2) and the relations (3) were known for several years (10-12). In terms of the nomenclature of Madey and Pflumm (12), the transmission through a bed with length  $L$  is

$$T = \frac{c}{c_0} = \frac{1}{2} \exp(\Delta^{-1}) \operatorname{erfc}(s_+) + \frac{1}{2} \operatorname{erfc}(s_-) \quad (4)$$

with

$$\text{Arguments: } s_{\pm} \equiv \frac{1}{2\Delta^{1/2}} \left[ \left( \frac{t_p}{t} \right)^{1/2} \pm \left( \frac{t}{t_p} \right)^{1/2} \right] \quad (5)$$

$$\text{Dispersion number: } \Delta \equiv D/uL \quad (6)$$

$$\text{Propagation time: } t_p \equiv \left[ \frac{(1 - \varepsilon)K'}{\varepsilon} + 1 \right] \frac{L}{u} \quad (7)$$

The time-dependent transmission function depends explicitly only on two parameters: the dispersion number  $\Delta$  and the propagation time  $t_p$ . These two parameters can be calculated from the transmission data by a numerical method described by Madey and Charles (13).

## EXPERIMENTAL PROCEDURES

The flow system, shown schematically in Fig. 1, is constructed of stainless-steel tubing and valves with Teflon seats and gaskets. Flow controllers FCA, FCB, and FCC enable independent settings of the gas flow rate from cylinders A, B, and He (helium). Rotameters RA, RB, RC, and RD give an approximate value of the flow rate. The flowmeter FM measures the flow rate with an accuracy of  $\pm 0.5\%$ . Three-way ball valves B1, B2, B3, and B4 can divert the flow to the electronic dual-channel mass-flow controller (Emerson Electric Co., Brooks Instrument Div. Model 5841-1A1CC) which controls the flow rate to  $\pm 1\%$ . Three-way ball valves B5, B6, and B7 enable mixing of up to three gas streams. Similar valves B8 and B9 permit two modes: (1) flow through the adsorber bed and (2) flow bypassing the adsorber bed. The latter configuration is applied for calibration and normalization purposes. The pressure drop across

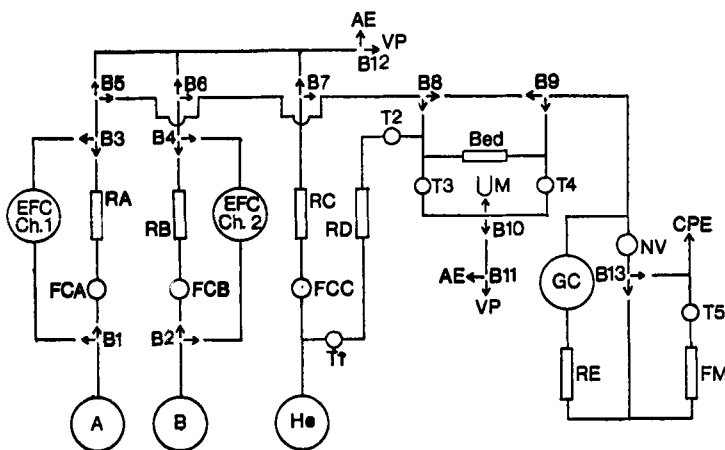


FIG. 1. Schematic diagram of the flow system.

the bed was measured by using the manometer M, and by appropriate manipulation of toggle valves T3 and T4. The automatic data acquisition system, located at the downstream side of the adsorber bed, consists of an automatic sampling valve (Carle Instruments Co. Model No. 4301), a Varian 3700 gas chromatograph with a flame ionization detector, and an Infotronics CRS-280 digital integrator. The data acquisition system measured the outlet concentration of contaminant gas at regular time intervals.

The cylindrical stainless-steel adsorber bed (30.13 cm long and 1.716 cm i.d.) was packed with 26.13 g of "Columbia" type 4LXC 12/28 activated carbon. This carbon has intrinsic density 1.560 g/cc (14), surface area 1130 m<sup>2</sup>/g (15), and pore volume 0.51 cc/g (15). Before measuring the mass of the carbon, the adsorber bed was desorbed at 200°C with helium flowing through the adsorber bed at a rate of 200 cc/min for 36 h. Also, after each run, the bed was desorbed for 12 h under the same temperature and helium flow conditions as above. The bed was immersed in a constant-temperature water bath which maintained the temperature within  $\pm 0.02^\circ\text{C}$  at 25°C. Repeated experiments verified the reproducibility of the results.

The gas mixture was prepared by a specialty gas supplier. The 105 ppm concentration of methane is known to within 1 %. Lower inlet concentrations of methane can be obtained by adding pure helium to the methane-helium mixture. Since the concentration of methane is small, one can assume that the mass flow rate is uniform through the bed. The total pressure in the adsorber bed ranged between 740 and 780 mmHg and the pressure drop ranged between 10 and 20 mmHg. The pressure drop is

small, and throughout this study we assume the gas flow rate is constant in the bed.

## RESULTS AND DISCUSSION

Listed in Table 1 are the measured transmissions of 105 ppm methane in helium at four different flow rates. Although the actual sampling intervals are 30 s, the two lower flow rates in Table 1 include only a portion of the data for convenience in tabulating. Dispersion numbers and propagation times were calculated by minimizing the sum of the squares of the errors between the experimental and the predicted transmissions (13). Values of the propagation times and the dispersion numbers are listed in Table 2 for 105 ppm methane in helium and some lower-concentration mixtures.

Propagation times can be calculated directly by integrating the transmission data. For any type of gas-solid equilibrium isotherm, the solid-phase concentration  $q_0$ , corresponding to the gas-phase concentration  $c_0$ , can always be calculated from the mass-balance equation

$$q_0(1 - \varepsilon)L + c_0\varepsilon L = uc_0\varepsilon \int_0^\infty [1 - T(t)] dt \quad (8)$$

Here the right-hand side represents the methane retained in the adsorber

TABLE I  
Transmissions of 105 ppm Methane-Helium Mixture at Different Flow Rates  
through Columbia 4LXC 12/28 Activated Carbon at 25°C

| $u = 0.687 \text{ cm/s}$ |                  | $u = 1.38 \text{ cm/s}$ |                  | $u = 2.70 \text{ cm/s}$ |                  | $u = 6.64 \text{ cm/s}$ |                  |
|--------------------------|------------------|-------------------------|------------------|-------------------------|------------------|-------------------------|------------------|
| Time $t$ (s)             | Transmission $T$ | Time $t$ (s)            | Transmission $T$ | Time $t$ (s)            | Transmission $T$ | Time $t$ (s)            | Transmission $T$ |
| 870                      | 0.0084           | 510                     | 0.0171           | 300                     | 0.0722           | 120                     | 0.0157           |
| 990                      | 0.0520           | 570                     | 0.0979           | 330                     | 0.2832           | 150                     | 0.6462           |
| 1110                     | 0.1508           | 630                     | 0.2776           | 360                     | 0.5884           | 180                     | 0.9837           |
| 1230                     | 0.3052           | 690                     | 0.5140           | 390                     | 0.8263           | 210                     | 0.9952           |
| 1350                     | 0.4845           | 750                     | 0.7279           | 420                     | 0.9414           | 240                     | 0.9963           |
| 1470                     | 0.6513           | 810                     | 0.8695           | 450                     | 0.9796           |                         |                  |
| 1590                     | 0.7825           | 870                     | 0.9438           | 480                     | 0.9899           |                         |                  |
| 1710                     | 0.8734           | 930                     | 0.9764           | 510                     | 0.9922           |                         |                  |
| 1830                     | 0.9293           | 990                     | 0.9878           | 540                     | 0.9933           |                         |                  |
| 1950                     | 0.9610           | 1050                    | 0.9915           |                         |                  |                         |                  |
| 2070                     | 0.9784           |                         |                  |                         |                  |                         |                  |
| 2190                     | 0.9863           |                         |                  |                         |                  |                         |                  |
| 2310                     | 0.9908           |                         |                  |                         |                  |                         |                  |

TABLE 2

Propagation Times, Dispersion Numbers, and Adsorption Capacities of Methane in the Columbia 4LXC 12/28 Activated Carbon Adsorber Bed at 25°C

| Methane concentration $x_0$ (ppm) | Interstitial flow velocity $u$ (cm/s) | Propagation time $t_p$ (s) | Dispersion number $\Delta \times 10^2$ | Dimensionless adsorption capacity <sup>a</sup> $K$ |
|-----------------------------------|---------------------------------------|----------------------------|--|--|
| 105                               | 0.687                                 | 1390                       | 2.02                                   | 71.7   |
| 105                               | 1.38                                  | 694.6                      | 1.08                                   | 71.7   |
| 105                               | 2.70                                  | 353.9                      | 0.618                                  | 71.7   |
| 105                               | 6.64                                  | 145.6                      | 0.416                                  | 72.6   |
| 85                                | 0.690                                 | 1386                       | 1.99                                   | 71.8   |
| 34                                | 0.690                                 | 1385                       | 1.89                                   | 71.8   |

<sup>a</sup>Values of  $K$  are based on  $\epsilon_p = 0.443$  and  $\epsilon = 0.568$ , which come from Refs. 14 and 15.

bed. The first term on the left-hand side is the methane retained on the granules of the adsorbent; the second term is the methane in the interstitial regions.

Substituting the transmission Eq. (4) and performing the integration, we find [the definitions of  $K$  and  $c_0$  in this paper are not the same as in previous papers (3-6)]

$$q_0 = \frac{c_0 \epsilon}{(1 - \epsilon)} \left( \frac{ut_p}{L} - 1 \right) \quad (9)$$

Since  $q_0 = K'c_0$ , Eq. (9) becomes

$$ut_p = \frac{K'(1 - \epsilon)L}{\epsilon} + L \quad (10)$$

which is equivalent to Eq. (7). Although the procedure from Eq. (8) to Eq. (10) is not applicable when Eq. (4) is not valid, Eq. (8) may always be used for calculating the values of  $K$ ,  $K'$ , and  $q_0$ .

Equation (10) gives the relation between two dynamic properties (viz.,  $u$  and  $t_p$ ) and other physical properties of the system (viz.,  $K'$ ,  $\epsilon$ , and  $L$ ). The adsorption capacities  $K'$  and  $K$  are similar to the partition coefficient in gas-liquid absorption studies in the sense that each is a ratio of two volume quantities (16); however, the values of  $K'$  and  $K$  depend on the surface area of the solid. Although a porous carbon with twice the specific area will have twice the  $K$  value, the value of  $K'$  will not be twice as large because it depends on the pore volume fraction  $\epsilon_p$ . For a given adsorber bed, Eq. (10) indicates that there is a reciprocal relation between flow rate and the propagation time. This relation can be applied to check the data at different flow rates.

Calculated  $K$  values for different flow rates and different methane concentrations are listed in Table 2. These values indicate that Eq. (10) holds except at the highest flow rate where only a few measurements were made. The constancy of  $K$  values for different methane concentrations shows also that the linear isotherm, Eq. (3), is valid for the concentration range of this study. Also, we performed a numerical integration on the transmission data of 105 ppm methane for the lowest flow rate. The numerical integration gives a propagation time of 1391 s, which agrees with the value in Table 1 and justifies the use of the simultaneous optimization of both  $\Delta$  and  $t_p$  by the method of Madey and Charles (13).

A more quantitative criterion on the equilibrium assumption, Eq. (3), can be made by using a different relation (10) between  $c$  and  $q$ :

$$\frac{dq}{dt} = k_c a(c - q/K') \quad (11)$$

This equation specifies that the time rate of change of solid-phase concentration is proportional to the product of a mass-transfer coefficient  $k_c$ , the specific exterior surface area  $a$  of solid particles, and the "driving force" which is represented by the difference between the gas-phase concentration  $c$  in the bulk flow and the concentration  $q/K'$  near the solid surface. The correlation of the mass-transfer coefficient  $k_c$  is given by Petrovic and Thodos (17) as

$$k_c = 0.357u \text{ Re}^{-0.359} \text{ Sc}^{-0.667} \quad (12)$$

where  $\text{Re}$  and  $\text{Sc}$  are the dimensionless Reynolds and Schmidt numbers, respectively. (The correlation was given for the equimolar counterdiffusion mass-transfer coefficient  $k'_c$ ; however, because the mole fraction of methane is small, we neglect the difference between  $k'_c$  and the mass-transfer coefficient  $k_c$  through the stationary gas phase.) The value of  $a$  for nearly-spherical particles can be estimated from (18)

$$a = \frac{6(1 - \varepsilon)}{d_p} \quad (13)$$

where  $d_p$  is the mean particle diameter.

Equation (11) then can be written in a dimensionless form:

$$\frac{1}{\alpha} \frac{d(q/q_0)}{d(t/t_p)} = \frac{c}{c_0} - \frac{q}{K'c_0} \quad (14)$$

Here

$$\alpha = k_c a t_p / K' = 2.14(1 - \varepsilon) \left[ \frac{1 - \varepsilon}{\varepsilon} + \frac{1}{K'} \right] L d_p^{-1} \text{ Re}^{-0.359} \text{ Sc}^{-0.667} \quad (15)$$

The dimensionless quantity  $\alpha$  is a factor that represents the relative speed between the interphase mass transfer rate and the longitudinal moving rate of the adsorbed component. Note that Eq. (14) is a first-order differential equation; any change of gas-phase concentration will change the solid-phase concentration at a speed proportional to  $\alpha$ . At a time equal to the propagation time  $t_p$ , the difference in the solid-phase concentration from the equilibrium value is given by the factor  $\exp(-\alpha)$ . In order to reach equilibrium quickly,  $\alpha$  must be large, which corresponds to small mass-transfer resistance. In the limiting case when  $\alpha \rightarrow \infty$ ,  $q$  will be equal to  $K'c_0$  and the equilibrium assumption is attained. Because  $\alpha$  is a function of the Reynolds number, it decreases with increasing superficial flow velocity. The values of  $\alpha$ , listed in Table 3, are far greater than unity. Thus, even allowing for some uncertainties in the use of Eqs. (12) and (13), we find that the equilibrium assumption is valid for this study.

After establishing the linear equilibrium assumption, we compared the time-dependent transmission data with Eq. (4). We plot the experimental data in Fig. 2, which gives the dimensionless transmission  $c/c_0$  versus the dimensionless time  $t/t_p$  for the four flow rates listed in Table 1. These data agree with the predicted curves which were calculated using the dispersion numbers in Table 2. It is clearly seen that the transmission curves become more diffuse as the flow rate decreases. Note that a diffuse curve does not necessarily relate to a high effective diffusion coefficient; in fact, the value of the effective diffusion coefficient increases when the flow rate increases, but the dispersion number decreases. The reason that a high-velocity flow results in a steeper transmission curve is clear when the propagation time is taken into consideration. For a high-velocity

TABLE 3  
Effective Diffusion Coefficients, Reynolds Numbers, and Values of  $\alpha$  in the  
4LXC 12/28 Activated Carbon Adsorber Bed at 25°C

| Methane concentration $x_0$ (ppm) | Interstitial flow velocity $u$ (cm/s) | Effective diffusion coefficient $D$ (cm <sup>2</sup> /s) | Reynolds <sup>a</sup> numbers $\times 10^2$ | Relative <sup>b</sup> speed factor $\alpha$ |
|-----------------------------------|---------------------------------------|--|---|---|
| 105                               | 0.687                                 | 0.313  | 9.6   | 266   |
| 105                               | 1.375                                 | 0.334  | 19.3  | 272   |
| 105                               | 2.70                                  | 0.376  | 37.8  | 214   |
| 105                               | 6.64                                  | 0.623  | 93.0  | 155   |
| 85                                | 0.690                                 | 0.310  | 9.6   | 266   |
| 34                                | 0.690                                 | 0.294  | 9.6   | 266   |

<sup>a</sup>Reynolds numbers were calculated using  $d_p = 0.14$  cm and  $\mu = 2.0 \times 10^{-4}$  g/cm/s.

<sup>b</sup>Values of  $\alpha$  are based on  $Sc = 1.59$ . Both the viscosity  $\mu$  and the mutual diffusion coefficient  $D_{12}$  are calculated according to a standard method (21).

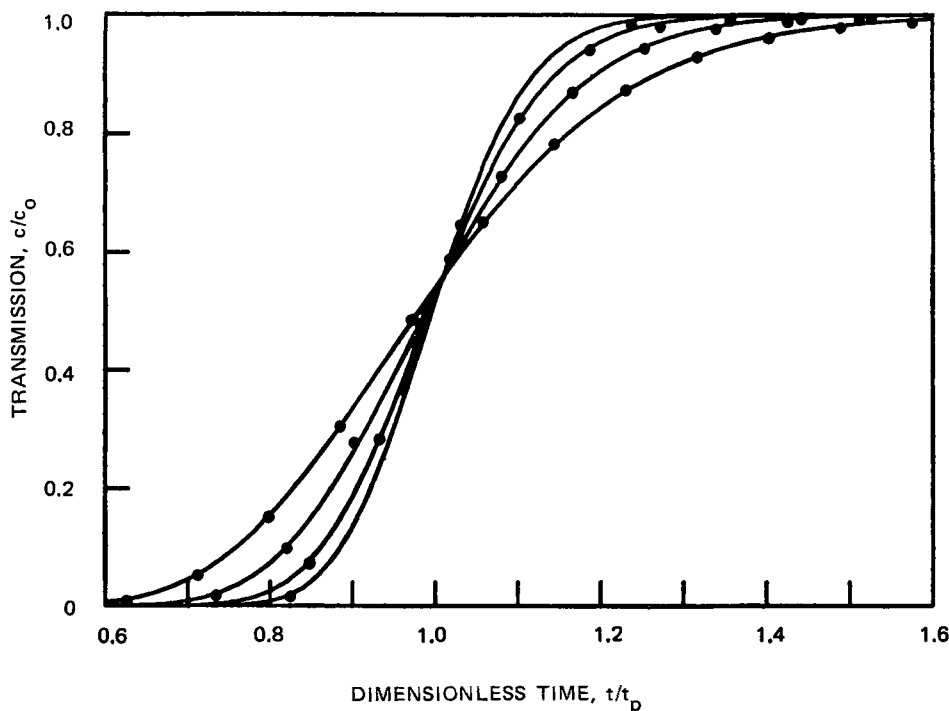


FIG. 2. Transmission versus dimensionless time for four flow rates. Points are experimental results listed in Table 1. Solid curves are predicted results based on Eq. (4). The flow rates, which increase with the steepness of the curves, are 0.687, 1.375, 2.70, and 6.64 cm/s, respectively.

flow, the propagation time is so small that the concentration distribution of the trace component changes only slightly from the step input function; therefore, in discussing the shape of transmission curves, the dispersion number is a better parameter than the effective diffusion coefficient.

The increase of the effective diffusion coefficient with increasing flow rate was recognized from the Taylor dispersion formula (19) which gives the value of  $D$  of the trace component flowing through an empty tube. The modification of the Taylor dispersion formula to a packed tube was made by Van Deemter et al. (9). His equation has the general form

$$H = \frac{L}{N} = A + \frac{B}{u} + Cu \quad (16)$$

where  $H$  is the height equivalent to the theoretical plate (H.E.T.P.) and  $N$  is the number of theoretical plates. Constants  $A$ ,  $B$ , and  $C$  in Eq. (12)

represent the contribution of dispersion from different sources (9, 16). The constant  $A$  is the eddy diffusion coefficient resulting from different paths in the packed bed,  $B$  is the Brownian motion of the trace gas in the carrier gas, and  $C$  is the contribution of the mass-transfer resistance.

It has been pointed out by Lee and Madey (20) that the plate theory of Glueckauf (11) is similar to the differential equation method, and that the following equation relates the number  $N$  of theoretical plates and the dispersion number  $\Delta$ :

$$\Delta = 1/2N \quad (17)$$

It is obvious from Eq. (17) that the flow rate dependence of the dispersion number has the same functional form as Eq. (16). The fact that the dispersion number decreases with flow rate in this study confirms the assumption that the mass-transfer resistance is not important since otherwise the dispersion number would increase.

## CONCLUSION

We measured the transmission of low concentrations of methane in a helium carrier-gas flow. Data were compared with the Madey-Pflumm equation and shown to be in good agreement. The linear equilibrium assumption was tested both by comparing the adsorption capacities and by examining the mass-transfer resistance. The conclusion from the present investigations is that the equation and the underlying assumption are adequate for the concentration and the flow rate regions of this study.

## SYMBOLS

- $a$  specific exterior area of carbon granules
- $A, B, C$  constants in Van Deemter equation
- $c$  gas phase concentration of the contaminant
- $D$  effective diffusion coefficient
- $D_{12}$  mutual diffusion coefficient of the contaminant gas and the carrier gas
- $d_p$  averaged diameter of carbon granules
- $H$  height equivalent to the theoretical plate
- $K$  true adsorption capacity. The volume of gas adsorbed per unit volume of the solid absorbent (which does not include the pore volume)
- $K'$  apparent adsorption capacity. The volume of gas adsorbed per unit volume of the adsorbent (which includes the pore volume but not the interstitial volume)

|                 |   |
|-----------------|---|
| $k_c$           | mass-transfer coefficient through the nondiffusing gas phase  |
| $k'_c$          | equimolal counterdiffusion mass-transfer coefficient  |
| $L$             | length of the bed   |
| $N$             | number of the theoretical plate   |
| $q$             | the average concentration of the contaminant gas in the adsorbent which includes the pore volume. The unit of $q$ is mole per unit volume of adsorbent granules |
| $Re$            | Reynolds number ( $\equiv ud_p\rho/\mu$ )   |
| $s_{\pm}$       | argument defined in Eq. (5)   |
| $t$             | time  |
| $t_p$           | propagation time  |
| $T$             | transmission ( $\equiv c/c_0$ )   |
| $u$             | interstitial flow velocity  |
| $Sc$            | Schmidt number [ $\equiv(\mu/\rho)D_{12}$ ]   |
| $x_0$           | mole fraction of the contaminant gas  |
| $z$             | coordinate of bed length  |
| $\alpha$        | dimensionless relative speed factor defined in Eq. (15)   |
| $\varepsilon$   | void volume fraction external to the adsorbent granules   |
| $\varepsilon_p$ | pore volume fraction within the granules of the adsorbent   |
| $\Delta$        | dispersion number   |
| $\mu$           | viscosity of the gas mixture  |
| $\rho$          | density of the gas mixture  |

## Acknowledgment

This work was supported in part by the Department of Energy under contract DE-AC02-80ER10622.

## REFERENCES

1. J. C. Giddings, *Dynamics of Chromatography*, M. Dekker, New York, 1965.
2. A. V. Kiseler and Y. Z. Yashin, *Gas-Adsorption Chromatography* (translated by J. E. S. Bradley), Plenum, New York, 1969.
3. R. Madey, P. J. Photinos, and K. B. Lee, *Nucl. Sci. Eng.*, **67**, 269 (1978).
4. R. Madey and P. J. Photinos, *Carbon*, **17**, 93 (1979).
5. R. Forsythe, M. Czayka, R. Madey, and J. Povlis, *Ibid.*, **16**, 27 (1978).
6. P. J. Photinos, A. Nordstrom, and R. Madey, *Ibid.*, **17**, 506 (1979).
7. R. J. Hamilton and P. A. Sewell, *Introduction to High Performance Liquid Chromatography*, Chapman and Hall, London, 1977.
8. W. Rieman III and H. F. Walton, *Ion Exchange in Analytical Chemistry*, Pergamon, New York, 1970.
9. J. J. Van Deemter, F. J. Zuiderweg, and A. Klinkenberg, *Chem. Eng. Sci.*, **5**, 271 (1956).
10. L. Lapidus and N. R. Amundson, *J. Phys. Chem.*, **56**, 984 (1952).
11. E. Glueckauf, *Trans. Faraday Soc.*, **51**, 34 (1955).

12. R. Madey and E. Pflumm, *A Physical Theory of Adsorption*, Unpublished Report RAC-885, Republic Aviation Corp., 1962.
13. R. Madey and J. Charles, "The Transmission of Carbon-Dioxide through Molecule Sieve Adsorption Beds," Paper Presented at the 64th National Meeting of the American Institute of Chemical Engineers, New Orleans, Louisiana, March 16-20, 1969.
14. K. B. Lee, PhD Dissertation, Department of Physics, Clarkson College of Technology, Potsdam, New York, 1971.
15. M. Manes, Department of Chemistry, Kent State University, Private Communication.
16. R. J. Laub and R. L. Pecsok, *Physicochemical Applications of Gas Chromatography*, Wiley, New York, 1978.
17. L. J. Petrovic and G. Thodos, *Ind. Eng. Chem., Fundam.*, 7, 274 (1968).
18. J. M. Coulson and J. F. Richardson, *Chemical Engineering*, Vol. 2, 2nd ed., Pergamon, New York, 1964.
19. G. Taylor, *Proc. R. Soc.*, A219, 186 (1953).
20. K. B. Lee and R. Madey, *Trans. Faraday Soc.*, 67, 329 (1971).
21. R. B. Bird, W. E. Stewart, and E. N. Lightfoot, *Transport Phenomena*, Wiley, New York, 1960, pp. 23, 511.

*Received by editor September 25, 1980*